Electronic Supplementary Information

Photocatalytic water oxidation over $LaWO_{0.6}N_{2.4}$ mesoporous single crystals under visible and near-infrared light illumination

Lin Yang,[a] Hui Duan*[a] and Xiaoxiang Xu*[a]

Shanghai Key Lab of Chemical Assessment and Sustainability, School of Chemical Science & Engineering, Tongji University, Shanghai, 200092, China

*Corresponding authors

Hui Duan (Email: dhui@tongji.edu.cn, Tel: +86-21-65982670)

Xiaoxiang Xu (Email: xxxu@tongji.edu.cn, Tel: +86-21-65986919)

Supporting information content

Number of pages: 15 (S1-S16)

Number of figures: 10 (Figure S1-S10)

Number of tables: 5 (Table S1-S5)

Content

Figures:

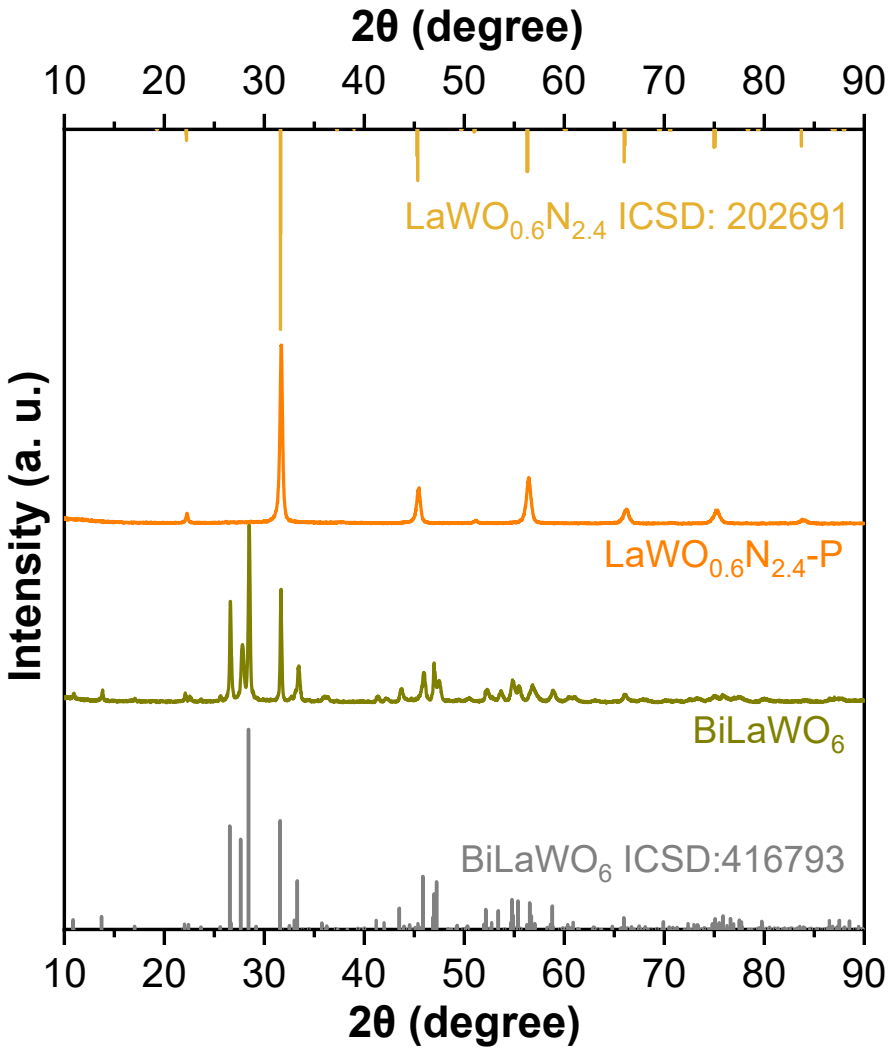

Fig. S1. XRD patterns for $BiLaWO_6$ and $LaWO_{0.6}N_{2.4}$-P, standard patterns of $BiLaWO_6$ and $LaWO_{0.6}N_{2.4}$ are also included for comparisons.

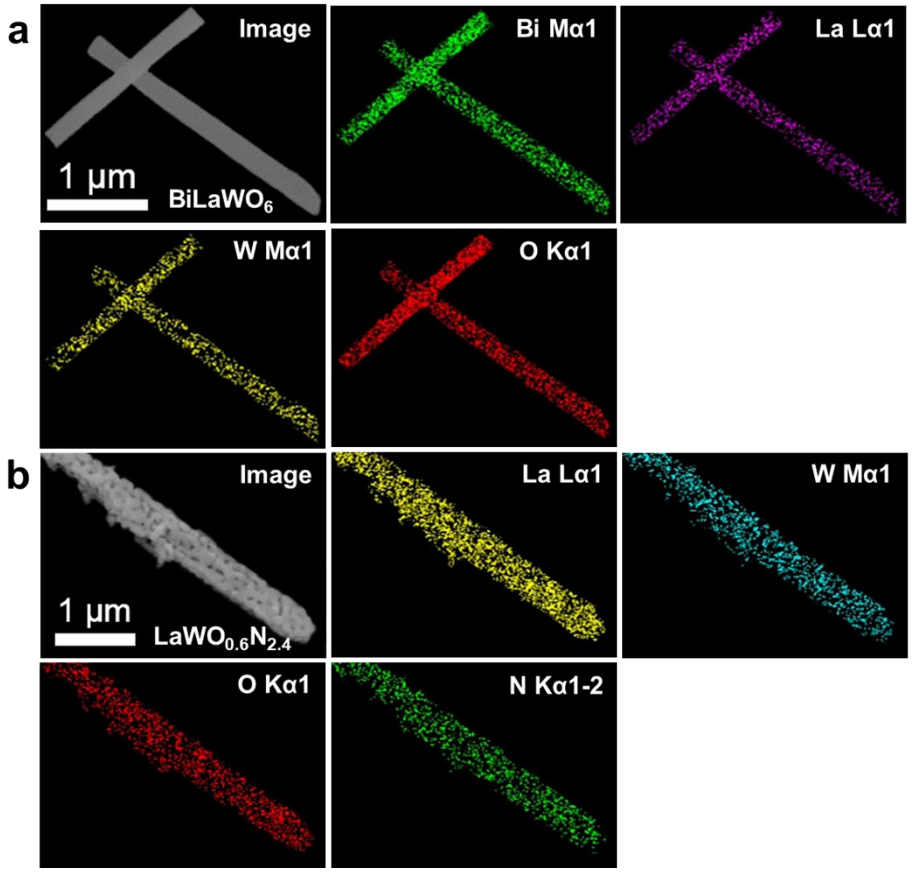

Fig. S2. FE-SEM images and corresponding SEM-EDS elemental mapping images for (a) $BiLaWO_6$ and (b) $LaWO_{0.6}N_{2.4}$-P.

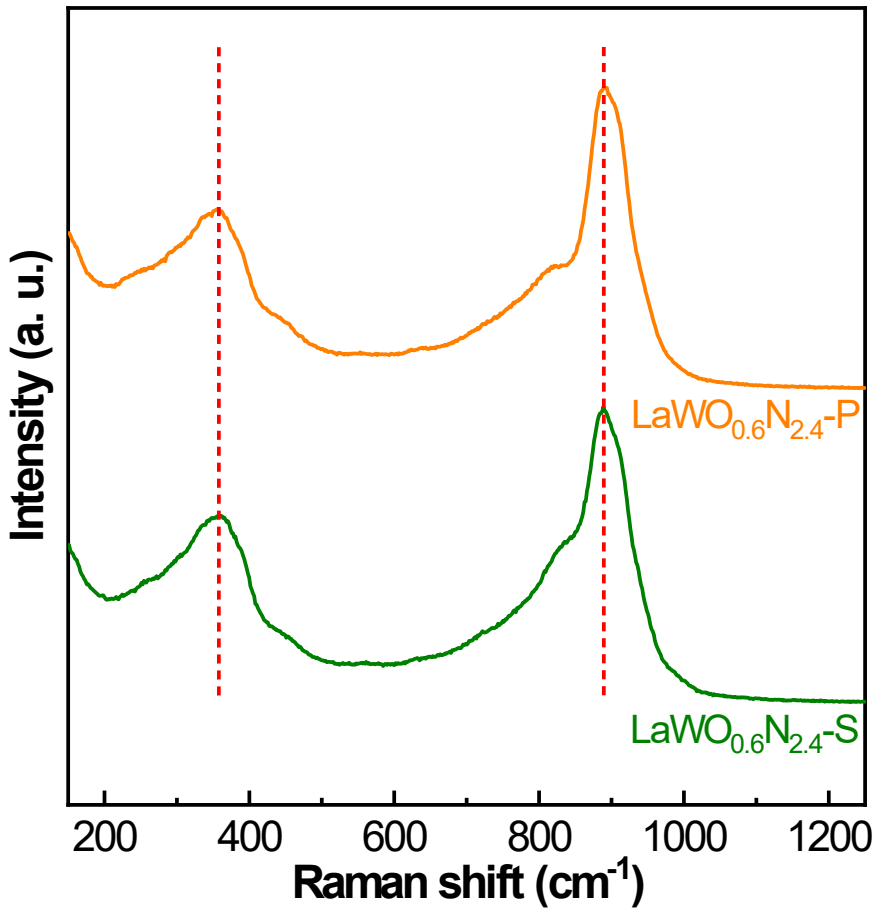

Fig. S3. Raman spectra for freshly prepared sample powders of $LaWO_{0.6}N_{2.4}$-S and $LaWO_{0.6}N_{2.4}$-P.

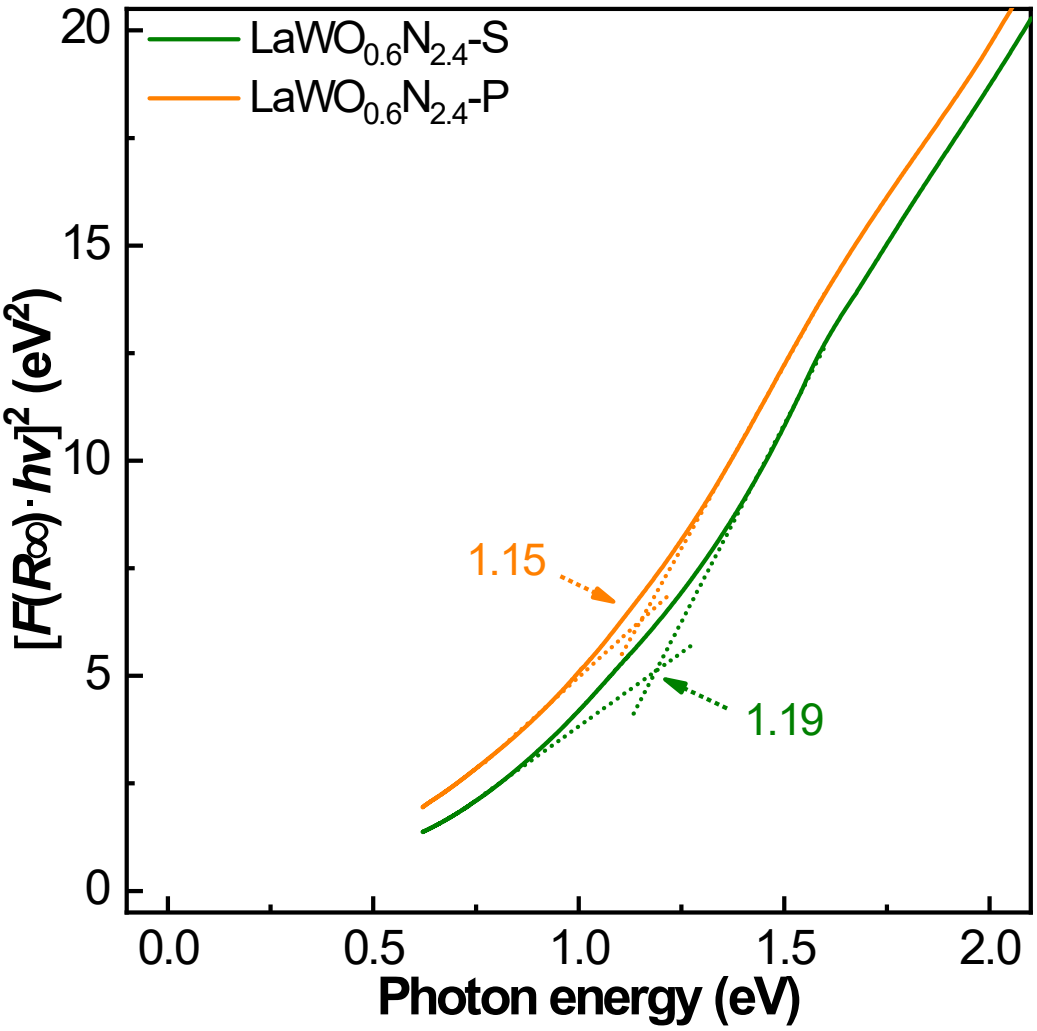

Fig. S4. Tauc plot for $LaWO_{0.6}N_{2.4}$-S and $LaWO_{0.6}N_{2.4}$-P; bandgap values are assessed by a modified Tauc method owing to the high defect's absorption background.[1]

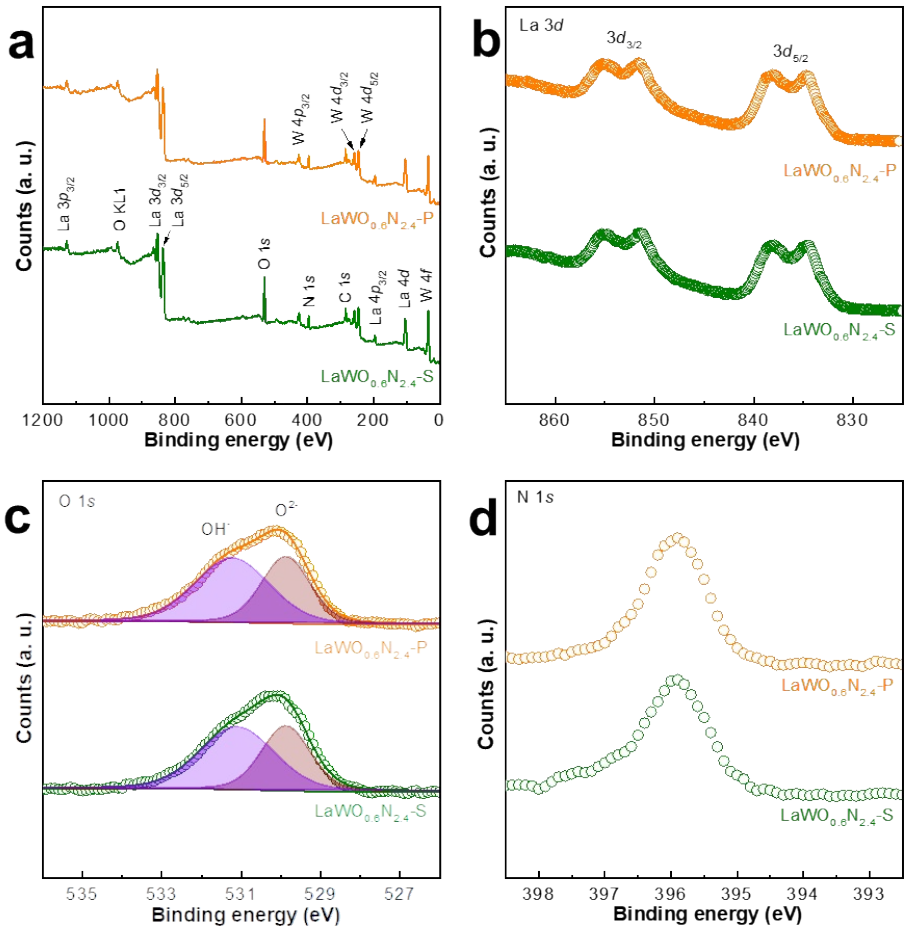

Fig. S5. XPS analyses for $LaWO_{0.6}N_{2.4}$-S and $LaWO_{0.6}N_{2.4}$-P: (a) survey spectra; (b) La 3*d*; (c) O 1*s* and (d) N 1*s* regions.

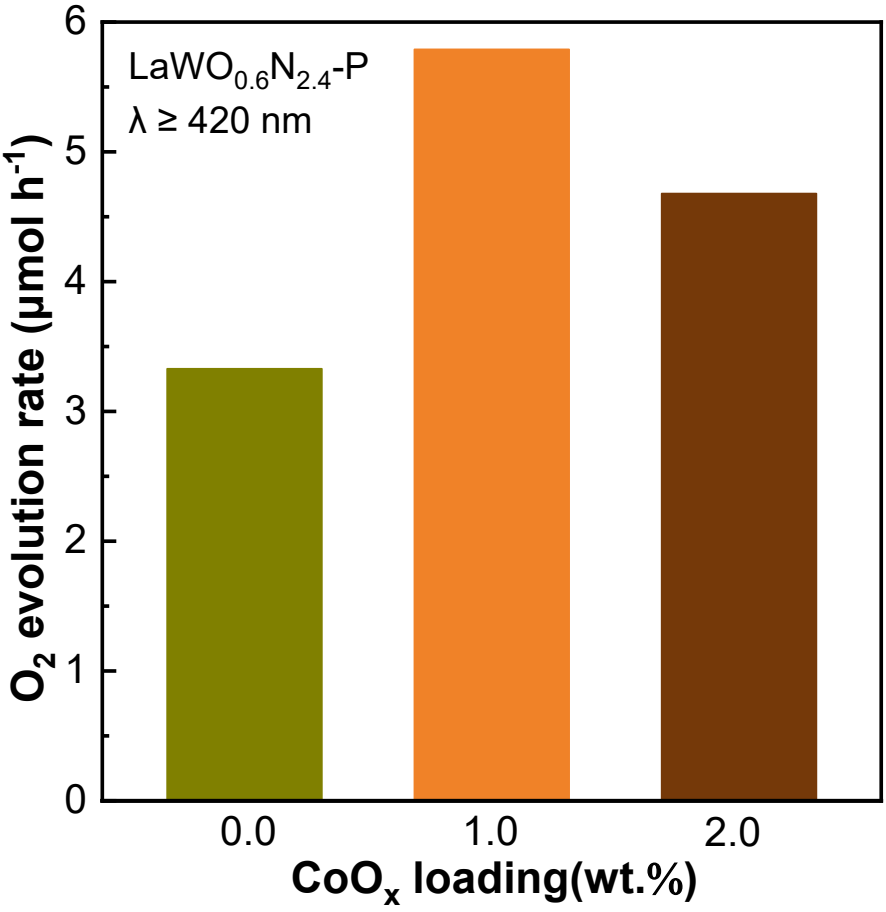

Fig. S6. Temporal O_2 evolution over $LaWO_{0.6}N_{2.4}$-P with different CoO_x content under visible light illumination ($\lambda \geq 420$ nm) in 0.05 M $AgNO_3$ aqueous solution containing 0.2 g La_2O_3 (pH buffer).

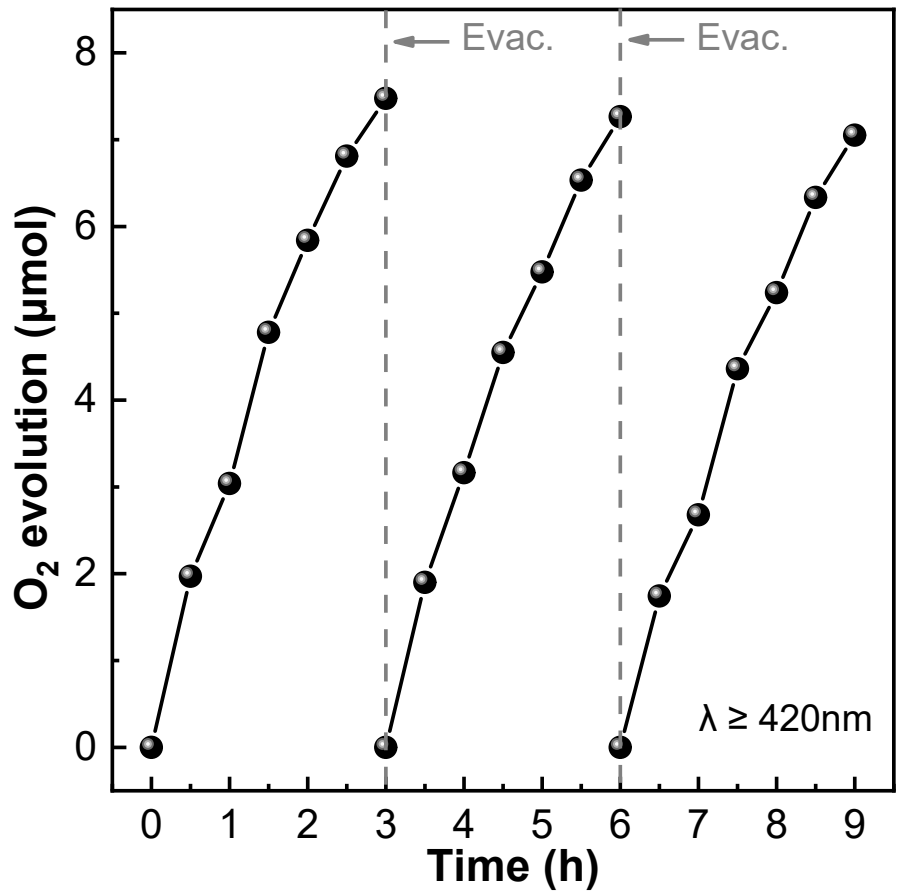

Fig. S7. Repeated photocatalytic oxygen evolution test for $LaWO_{0.6}N_{2.4}$-P loaded with 1 wt.% CoO_x under visible light illumination ($\lambda \geq 420$ nm) in 0.05 M sodium persulfate aqueous solution.

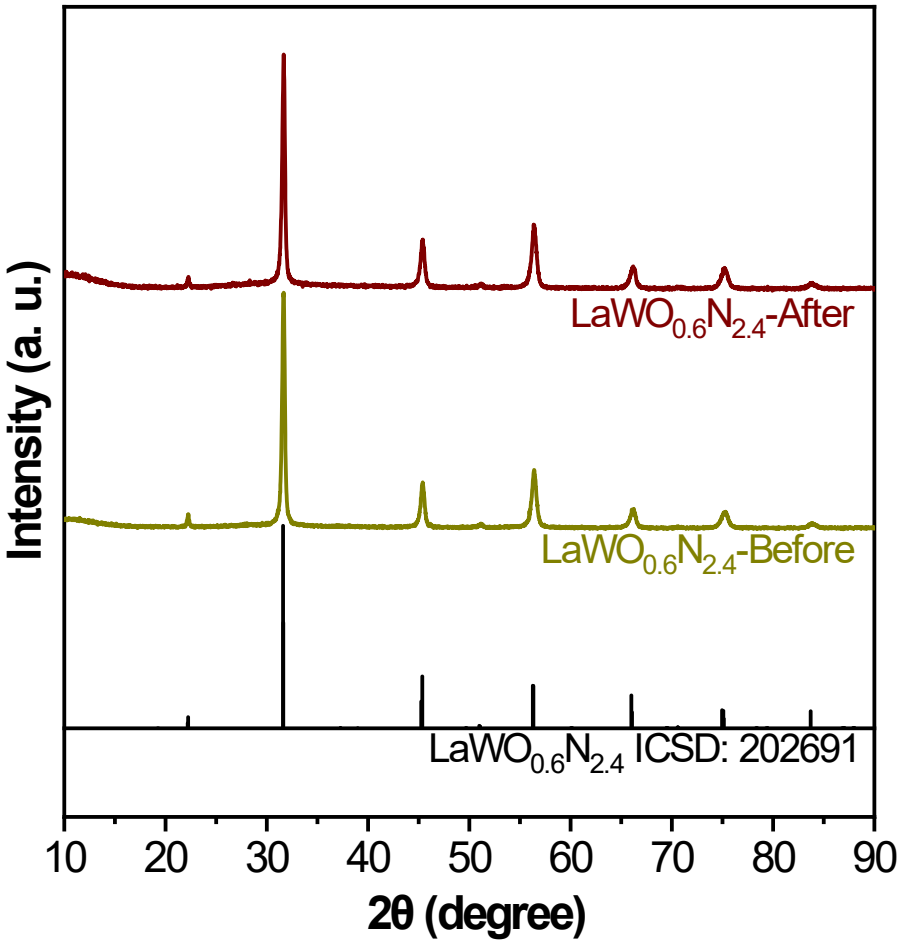

Fig. S8. XRD powder diffraction patterns for $LaWO_{0.6}N_{2.4}$-P before and after photocatalytic water oxidation (OER) examination. Standard patterns of $LaWO_{0.6}N_{2.4}$ is also included for clarity.

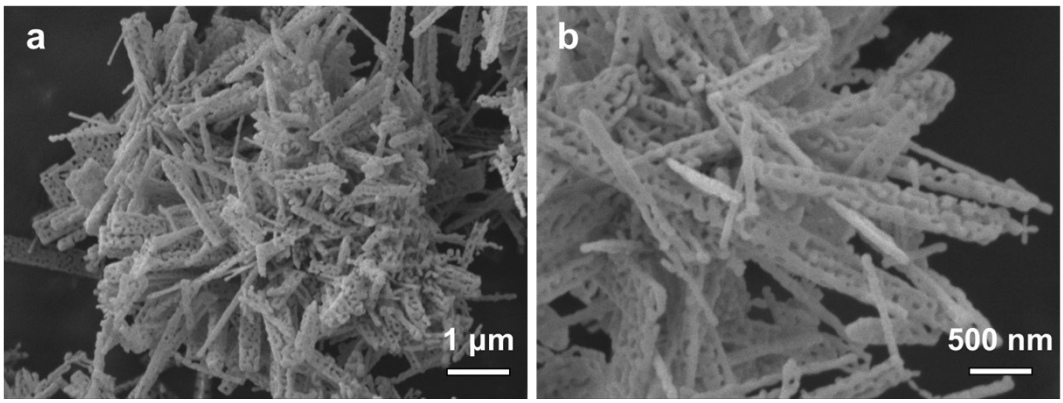

Fig. S9. FE-SEM images for $LaWO_{0.6}N_{2.4}$-P after photocatalytic water oxidation reaction under different magnifications.

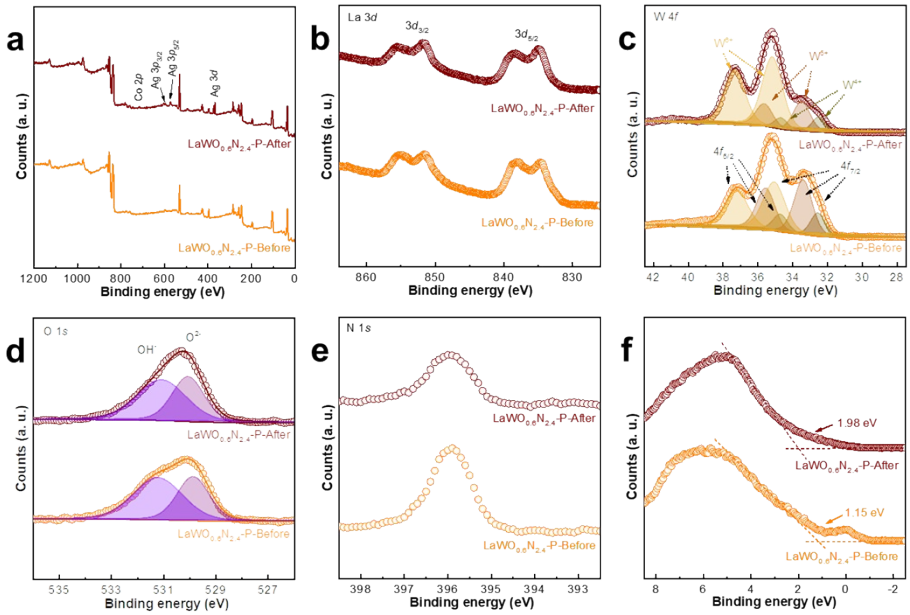

Fig. S10. X-ray photoelectron spectroscopy (XPS) analysis for $LaWO_{0.6}N_{2.4}$-P before and after photocatalytic experiment: (a) Survey scan; (b) La 3*d*; (c) W 4*f*; (d) O 1*s*; (e) N 1*s*; (f) XPS valence band scan. Ag signal detected can be attributed to the photo-reduction of $AgNO_3$ sacrificial agent.

Table S1. Refined unit cell parameters and bandgap values for sample powders of $LaWO_{0.6}N_{2.4}$-S and $LaWO_{0.6}N_{2.4}$-P (standard deviations in parentheses).

Sample	*S.G.*	*a* (Å)	*b* (Å)	*c* (Å)	*α* (°)	*β* (°)	*γ* (°)	*V* (Å^3)
$BiLaWO_6$	*A*12/*m*1	8.3037(5)	3.8699(8)	16.4552(4)	90.000(0)	102.016(3)	90.000(0)	517.210(0)
$LaWO_{0.6}N_{2.4}$-P	*I*4-	5.6457(4)	5.6457(4)	7.9986(1)	90.000(0)	90.000(0)	90.000(0)	254.948(1)

**S.G.*: space group; *a*, *b*, and *c*: lengths of cell edges; *α*, *β*, and *γ*: angles respectively formed by *b* and *c, c* and *a*, and *a* and *b* edges; *V*: unit cell volume.

Table S2. Element composition in $LaWO_{0.6}N_{2.4}$-S and $LaWO_{0.6}N_{2.4}$-P determined by ICP-OES analysis and oxygen-nitrogen-hydrogen analyzer, associated with calculated effective chemical formula.

Sample	La (wt%)	W (wt%)	O (wt%)	N (wt%)	Effective chemical formula
$LaWO_{0.6}N_{2.4}$-S	37.92	50.19	3.90	7.99	$LaWO_{0.90}N_{2.10}$
$LaWO_{0.6}N_{2.4}$-P	37.89	50.15	3.27	8.69	$LaWO_{0.79}N_{2.21}$

Table S3. BET surface area and BJH desorption average pore diameter of samples $LaWO_{0.6}N_{2.4}$-S and $LaWO_{0.6}N_{2.4}$-P.

Sample	BET surface area (m^2/g)	BJH desorption average pore diameter (nm)
$LaWO_{0.6}N_{2.4}$-S	4.1(1)	20.6(6)
$LaWO_{0.6}N_{2.4}$-P	7.5(3)	31.4(2)

Table S4. Peak fitting results of XPS data for $LaWO_{0.6}N_{2.4}$-S, $LaWO_{0.6}N_{2.4}$-P, and $LaWO_{0.6}N_{2.4}$-P after photocatalytic water oxidation examinations.

Sample	Element state	FWHM (eV)	Binding energy (eV)	Area	Content (at%)
$LaWO_{0.6}N_{2.4}$-S	La 3*d* (La^{3+})	--	--	--	15.90
	W $4f_{7/2}$ (W^{6+})	1.56	35.17	18916.18	4.12
	W $4f_{7/2}$ (W^{5+})	1.31	33.43	13249.31	2.89
	W $4f_{7/2}$ (W^{4+})	1.06	32.50	8461.90	1.84
	W $4f_{5/2}$ (W^{6+})	1.56	37.32	14187.13	3.09
	W $4f_{5/2}$ (W^{5+})	1.31	35.58	9937.06	2.17
	W $4f_{5/2}$ (W^{4+})	1.06	34.65	6346.43	1.37
	N 1s (N^{3-})	--	--	--	18.40
	O 1s (OH^-)	2.22	531.09	33398.72	29.94
	O 1s (O^{2-})	1.45	529.87	22622.10	20.28
$LaWO_{0.6}N_{2.4}$-P	La 3*d* (La^{3+})	--	--	--	15.21
	W $4f_{7/2}$ (W^{6+})	1.49	35.05	19346.68	3.79
	W $4f_{7/2}$ (W^{5+})	1.24	33.40	18146.62	3.55
	W $4f_{7/2}$ (W^{4+})	0.99	32.56	6144.71	1.21
	W $4f_{5/2}$ (W^{6+})	1.49	37.20	14510.01	2.84
	W $4f_{5/2}$ (W^{5+})	1.24	35.55	13609.96	2.67
	W $4f_{5/2}$ (W^{4+})	0.99	34.71	4608.53	0.91
	N 1s (N^{3-})	--	--	--	20.36
	O 1s (OH^-)	2.22	531.22	38399.59	29.39
	O 1s (O^{2-})	1.45	529.87	26218.87	20.07
$LaWO_{0.6}N_{2.4}$-P-After test	La 3*d* (La^{3+})	--	--	--	13.61
	W $4f_{7/2}$ (W^{6+})	1.39	35.16	28327.70	5.23
	W $4f_{7/2}$ (W^{5+})	1.14	33.48	9701.35	1.79
	W $4f_{7/2}$ (W^{4+})	0.89	32.52	3799.47	0.70
	W $4f_{5/2}$ (W^{6+})	1.39	37.31	21245.78	3.92
	W $4f_{5/2}$ (W^{5+})	1.14	35.63	7276.01	1.35
	W $4f_{5/2}$ (W^{4+})	0.89	34.67	2899.60	0.53
	N 1s (N^{3-})	--	--	--	12.88
	O 1s (OH^-)	2.22	531.07	45688.25	34.80
	O 1s (O^{2-})	1.45	530.06	33063.63	25.19

Table S5. The photon flux and O_2 evolution rate at specific monochromatic light.

λ (nm)	Flux (μmol·h^{-1})	O_2 evolution (μmol·h^{-1})
420 ± 20	1147	1.161
450 ± 35	1255	1.359
500 ± 35	1925	1.550
550 ± 35	2447	1.578
600 ± 40	2895	1.643
700 ± 20	1482	0.633
800 ± 20	770	0.250

Reference

1. B. Moss, Q. Wang, K. T. Butler, R. Grau-Crespo, S. Selim, A. Regoutz, T. Hisatomi, R. Godin, D. J. Payne, A. Kafizas, K. Domen, L. Steier and J. R. Durrant, Linking in situ charge accumulation to electronic structure in doped $SrTiO_3$ reveals design principles for hydrogen-evolving photocatalysts, *Nat. Mater.*, 2021, **20**, 511-517.